Proceedings of ENCIT 2016 16th Brazilian Congress of Thermal Sciences and Engineering

November 07-10th, 2016, Vitória, ES, Brazil

SIMULATION OF AN INTERNAL COMBUSTION ENGINE USING ECFM-3Z COMBUSTION MODEL IN A CFD 3D COMMERCIAL CODE COMPARED TO EXPERIMENTAL RESULTS

Leonardo Fonseca, leofonseca@ufmg.br
Raphael Braga, raphaelmeirelesb@gmail.com
Luiz Fernando Morais, luizfernando_cks@hotmail.com
Rudolf Huebner, rudolf@ufmg.br
Ramon Molina Valle, ramon@demec.ufmg.br
CTM – UFMG (Mobility Technology Center – Federal University of Minas Gerais), 6627 Antonio Carlos Av, Belo Horizonte, 31.270-000, Brazil
PPGMEC – UFMG (Post Graduation Program on Mechanical Engineering – Federal University of Minas Gerais), 6627 Antonio Carlos Av, Belo Horizonte, 31.270-000, Brazil

Abstract. This paper presents the results of simulation of an internal combustion engine using Extended Coherent Flame Model – 3 Zones (ECFM-3Z) combustion model in a Computational Fluid Dynamics (CFD) 3D commercial code, compared to experimental results for the same engine. The commercial code solves equations for conservation of mass, momentum, energy, RNG k-ε turbulence model, coupled with a model for near wall flow field, using the finite volume method. The 3D mesh model involves the internal volume of the cylinder, intake and exhaust ports, and takes into account the movement of the piston and valves by moving the mesh. It solves the mesh movement by adding and removing mesh layers in the cylinder, bellow and above valves. Grid independence studies are performed in order to make the results independent from the mesh. Mesh refinement is performed using characteristic length of the mesh at cylinder, intake and exhaust ports, so the characteristic length would be as close as possible the same for all regions. The ECFM-3Z model has empirical constants for adjustment, and so it needs experimental results not only for adjustment but also for validation. They are modified in order to make the results for in cylinder pressure, temperature, heat release rate and mass burned fraction as close as possible to the experimental ones. The model takes into account only one cylinder of the engine, which runs at 2100 rpm, 20% MBT and uses VVT. Results of the CFD model for two positions of VVT are compared to experimental ones for the conditions, in order to evaluate the behaviour of the combustion model under these conditions. The CFD results for in cylinder pressure for both cases are well correlated to experimental ones, although in cylinder temperature, heat release rate and mass burned fraction are not as well correlated.

Keywords*: Computational Fluid Dynamics, Internal Combustion Engines, ECFM-3Z, Engine 3D Modelling*

1. NOMENCLATURE

BDC	Bottom Dead Center	MAP	Manifold Air Pressure
CAD	Crank Angle Degrees	MBT	Maximum Break Tork
CFD	Computational Fluid Dynamics	RNG	ReNormalization Group
CFM	Coherent Flame Model	TDC	Top Dead Center
ECFM-3Z	Extended Coherent Flame Model – Three Zones	VVT	Variable Valve Train

2. INTRODUCTION

A major challenge for combustion scientists and engine development engineers is to optimize engine combustion for improved fuel economy and reduced exhausts emissions while maintaining outstanding performance, durability, and reliability at an affordable price (Millo et al., 2014; Alkidas, 2007; Drake and Haworth, 2007). One of the main strategies to reduce emissions is the use of alternative fuels, since they can be extracted from renewable resources, and their emission levels can be lower than traditional fossil-based fuels (Mardi et al., 2014).

Engine simulation models are valuable tools for engineers either working in the automotive industry or belonging to the research community, with the aim to design engines that comply with the strict emissions legislation while keeping high performance (Pariotis et al., 2011; Ge et al., 2009; Bernard et al., 2011). In the past 40 years, an enormous effort has been applied in the development of CFD 3D specific tools for simulating internal combustion engine complex phenomena, such as compressible flow through valves, injection of liquid or gaseous fuel and combustion of different types of fuels.

Among other models for combustion, the models of coherent flame have been proposed for modeling turbulent premixed flame. This modeling is particularly suited to the description of premixed flame combustion, which represents the main oxidation mechanism in spark ignition engines (Colin et al., 2003). The main advantage of this approach is to separate complex chemistry features, incorporated into the average flame speed, from turbulence/combustion interactions modeled by the flame surface density Σ (Poinsot and Veinant, 2001).

An extension of this model was proposed in 2003 for allowing the simulation of the two premixed combustion models: premixed flame and auto ignition flame (Colin et al., 2003). Another model was proposed in 2004, this time for general purpose use in simulation of internal combustion engines. The ECFM-3Z model keeps the unburned and burned gas zones

description of the ECFM model, as well as the premixed flame description based on the flame surface density equation (Colin and Benkenida, 2004). It also adds the possibility to take into account diffusion flame, while using a sub division of the cell to take into account different possible conditions of air and fuel in direct injection fuel engines.

In order to evaluate the results of a CFD 3D model, this paper presents the comparison between a commercial code and experimental results of an engine running with ethanol. The engine runs at 2100 rpm with 20% of throttle valve opening for two different valve train position. The ECFM-3Z combustion model is adjusted for each case and the results are compared to experimental ones.

2.1. ECFM-3Z Combustion Model

In ECFM-3Z model, the state of in cylinder gases is defined by variables Z and c, being Z mixture fraction variable and c the progress reaction variable (Colin and Benkenida, 2004). This way, the model is described in terms of mixture fraction and reaction progress as it is shown in Figure 1. The model was proposed by Colin and Benkenida as an extension of CFM (1999). The main characteristic of those models is the definition of a property of flow field Σ, which is the flame surface density, to calculate flame front propagation. This variable is defined by (1) (Colin et al., 2003) and its transport equation is defined by (2), as it is implemented in STAR-CD™ (CD-ADAPCO, 2013).

$$\Sigma = \frac{\delta A}{\delta V} \tag{1}$$

$$\frac{\partial \Sigma}{\partial t} + \nabla u_i \Sigma - \nabla\left[\left(\frac{\mu_t}{Sc_t} + D\right)\nabla\left(\frac{\Sigma}{\bar{\rho}}\right)\right] = \Sigma\left(C_{divu}\frac{2}{3}\nabla\vec{u} + C\alpha\Gamma\frac{\varepsilon}{k} + C\frac{2}{3}\frac{\rho_u}{\rho_b}U_l\Sigma\frac{1-c}{c} - \beta U_l\frac{\Sigma}{1-\bar{c}} - \frac{2}{3}\frac{1}{\gamma p}\frac{\partial p}{\partial t}\right) + S_{conv} \tag{2}$$

Equation (2) involves 11 terms directly, and some of those terms are defined by equations with 5 other terms, thus the complete explanation of these equations is left for the reader in references (Colin at al, 2003), (Colin and Benkenida, 2004) and (CD-ADAPCO®, 2013) for sake of brevity.

Among several semi empirical parameters that ECFM-3Z model involves, the most frequently used to adjust the model are α and β. Parameter α influences directly the term $C\alpha\Gamma\frac{\varepsilon}{k}$, which is a production term for flame surface density based turbulent stretching of the flame, but it also influences other terms once it is used for calculation of parameter C. Parameter β, for its instance, influences the term $\beta U_l\frac{\Sigma}{1-\bar{c}}$, which is a destruction term for flame surface density, but it also influences calculation of parameter C.

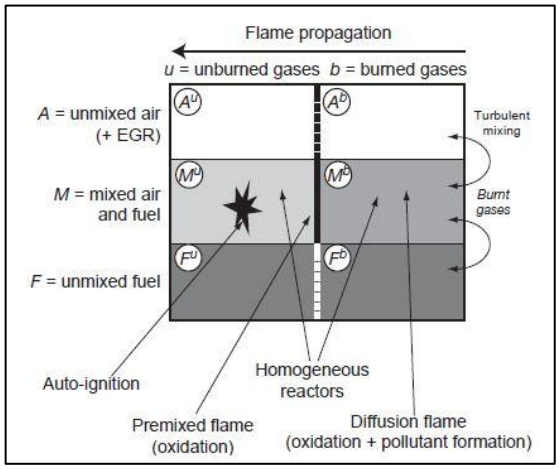

Figure 1 - Description of mixture fraction and reaction progress in ECFM-3Z model. SOURCE: (Colin and Benkenida, 2004).

It is the aim of this paper to perform the comparison between CFD and experimental results for different VVT positions using ECFM-3Z combustion model in a commercial code. Parameters such as in cylinder pressure versus crank angle, in cylinder temperature, heat release rate and mass burned fraction are compared with experimental ones in order to evaluate CFD model results.

3. ENGINE CFD 3D

The methodology of CFD simulation is usually described by the definition of volume of fluid that concerns the case studied, the generation of the mesh of finite volumes, the definition of physics and boundary conditions for the domain,

solution of the discretized equations and post processing the results. When it is applied to engines, this methodology must have slightly different approaches once the movements of piston and valves must be represented by some kind of movement of the mesh.

Many commercial codes, like STAR-CD™ for example, use strategies to add and remove mesh layers inside the domain each time the mesh elements become deformed over some limit, and those strategies depend on engine operation conditions.

A specific module for engine simulation receives as input the volume of fluid geometry of engine cylinder connected to intake and exhaust ports, and generates a database for grid movement during the entire engine cycle. This way it is possible to move the mesh while the program solves the equations for conservation of mass, momentum, energy and species, coupled to models for ideal gas, turbulence, combustion, injection of droplets in liquid phase, if any of those are necessary. Further description of software methodology can be found in specific documentation (CD-ADAPCO, 2013) and literature (Fonseca, 2014). The characteristics of CFD 3D model concerning geometry, grid independency and boundary conditions are briefly described on the next topics.

3.1. Geometry

The body of the text must be justified. The first line of each paragraph must be indented by 5 mm. Sufficient information must be provided directly in the text, or by reference to widely available published work. Footnotes should be avoided. All symbols and notation must be defined within the text. Physical quantities must be expressed in the SI (metric) units. Mathematical symbols appearing in the text must be typed in italic style.

The domain of the CFD 3D model is composed by the volume of one cylinder at the top dead center, along with intake and exhaust ports internal volume. The boundary conditions for inlet and outlet pressure are measured on the manifolds, so there will be a small amount of volume on both manifolds in order to introduce the boundary conditions on the correct position.

Figure 2 (a) shows the internal volume highlighted inside an assembly of an internal combustion engine, for illustrating the geometry of CFD 3D model and where it fits inside the engine. The result geometry for the engine 3D modeling is presented on Figure 2 (b).

The CFD 3D model consists in the volume of a two valve cylinder, which has dimensions of 70 mm bore and 86 mm stroke, swept volume of 331 cc(cubic centimeters). The combustion chamber is 27 cc, so it has a nominal compression ratio of 13.3:1. The cylinder geometry and valve events are presented on Table 1.

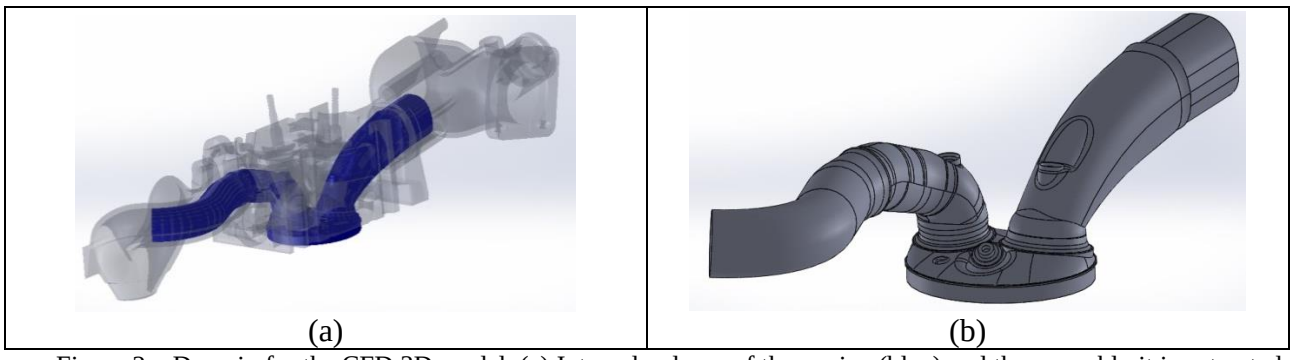

Figure 2 – Domain for the CFD 3D model. (a) Interval volume of the engine (blue) and the assembly it is extracted from; (b) CFD 3D model domain, concerning in cylinder volume, intake and exhaust ports.

Table 1 – Number of valves per cylinder for the engine under analyis.

Number of Valves	2

3.2. Grid Independency

In order to evaluate the influence of the mesh refinement on the overall results, a grid independency study was carried out. It was based on the methodology proposed by Celik et al. (2008), in which a characteristic length of the volumes is defined by equation 3 for a 2D grid and by equation 4 for a 3D grid.

$$h = \left[\frac{1}{N} \sum_{i=1}^{N} \left(\Delta A_i \right) \right]^{\frac{1}{2}} \tag{3}$$

$$h = \left[\frac{1}{N} \sum_{i=1}^{N} \left(\Delta V_i \right) \right]^{\frac{1}{3}} \tag{4}$$

In which ΔV_i is the volume, ΔA_i is the area of the cell and N is the total number of cells. Four grids were used starting from 1.0 mm and using a grid refinement factor ($r = h_{coarse} / h_{fine}$) of 1.1. Table 2 shows the four grids used with their respective characteristic length and the total number of cells in the bottom dead center (BDC) moment. In es-ICE, firstly a 2D template is built and based on that and some other parameters a 3D template is made. After that, the engine geometry is cut by this 3D template and an initial grid in each region is made. Then the assembly of the regions is done and, based on the events of the engine, a grid for each moment of the cycle is achieved. In this work, not only the 3D characteristic length was evaluated, but also the 2D characteristic length of the 2D template. In Appendix is shown the refinement in each template.

Three cycles of the engine were simulated in order to have a more established flow field and residuals gases. The value of α and β used were 1.0 for both variables and the time step for this analysis was 10^{-5}. Pressure, temperature and heat release rate comparison between different grids are shown in Figure 3. In the same figure, it is shown the computational time for the four grids simulated on this test.

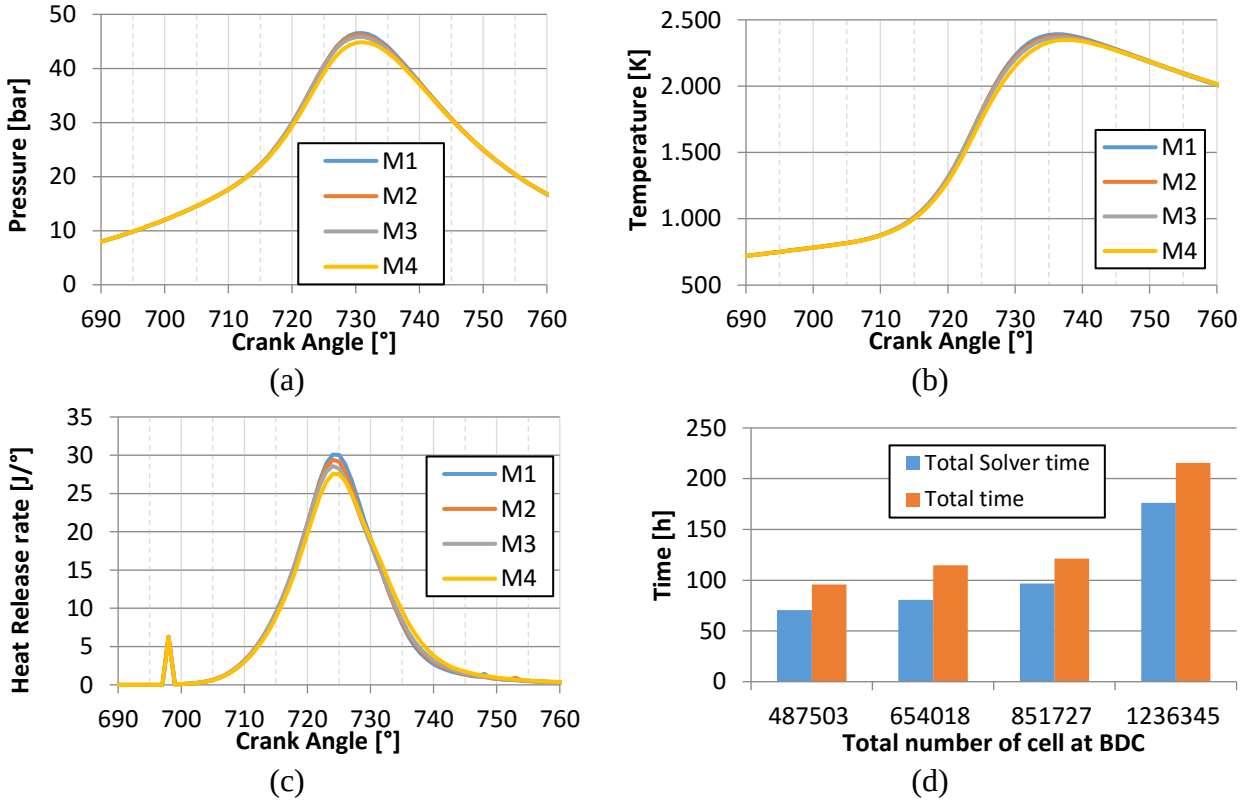

Figure 3 – Grid independence study results. (a) In-cylinder pressure curve for the four grids of the grid independency study; (b) In-cylinder temperature curve for the four grids of the grid independency study; (c) In-cylinder heat release rate curve for the four grids of the grid independency study; (d) Computational time for each grid of the grid independency study

The results showed a maximum relative difference between the meshes lower than 2.8%, 2.5% and 5.0% for pressure, temperature and heat release rate respectively. In addition, the computational cost for the finer grid was almost twice the computational time of the M3 grid. Based on that, the third grid (M3) was used for further analysis.

Table 2 – Grids used in the grid independency study with the corresponding characteristic length and total number of cells on BDC.

GRID	G1	G2	G3	G4
h_i [mm]	1.0	0.9	0.81	0.729
N	487,503	654,018	851,727	1,236,345

3.3. Cases and boundary conditions

This paper presents the results for simulation of two different cases with the engine running at 2100 rpm, 20% throttle. The first case runs with VVT 30 CAD, and the second one runs with VVT 60 CAD. VVT positions are defined as the interval between intake valve opening and exhaust valve closing, while both valves remain opened at the same time. A resume of both cases main information, along with valve timing, is presented at Table 3.

For both of them, boundary conditions at inflow and outflow are: pressure versus crank angle, temperature, turbulent intensity and turbulent length scale. Wall regions have no slip condition and zero pressure gradient, all of them. For temperature, they can have temperature set up, or be considered adiabatic, in such a manner that every wall which does not have temperature set up is considered adiabatic.

Table 3 – Cases for engine CFD 3D model.

	CASE 1	CASE 2
Engine speed	2100 rpm	2100 rpm
Intake pressure	71.8 kPa (20%)	73.6 kPa (20%)
Variable valve train (VVT)	30 CAD	60 CAD
Equivalence ratio (Lambda)	1.024	1.03
Spark timing	22.0 CAD BTDC	19.0 CAD BTDC
Intake valve opening	45[°] before TDC (315°)	15[°] before TDC (345°)
Intake valve closing	5 [°] before BDC (535°)	25 [°] after BDC (565°)
Exhaust valve opening	35 [°] before BDC (145°)	35 [°] before BDC (145°)
Exhaust valve closing	15[°] after TDC (375°)	15[°] after TDC (375°)

Boundary conditions for 2100 rpm, 20% throttle and 60 CAD VVT are presented following, and the boundary conditions for the other case are similar, with different values but no additional information. Intake and exhaust pressure versus crank angle are presented in Figure 4, temperature, turbulent intensity and length scale for the same region are presented in Table 4. Boundary conditions for wall temperature are presented in Table 5, in such a manner that the surfaces which does not have temperature defined are set adiabatic.

Initial conditions all of the regions composing the domain are presented at Table 6, for pressure, temperature, turbulent kinetic energy and turbulent kinetic energy dissipation.

Table 4 – Intake and exhaust boundary conditions for temperature, turbulent intensity and length scale, for Case 2.

	Intake	Exhaust
Temperature	311 K	769 K
Turbulent intensity	0.1	0.1
Length scale	0.0024 m	0.0017 m

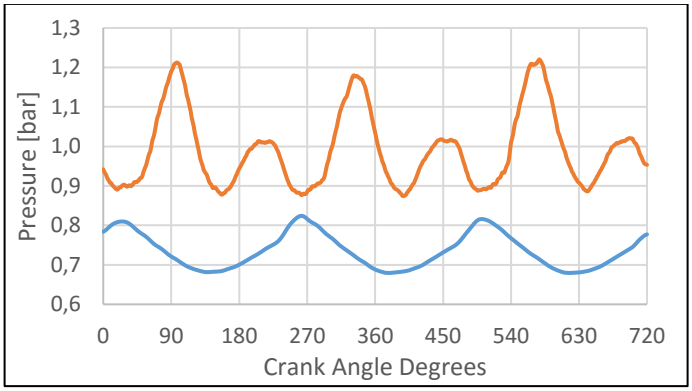

Figure 4 – Intake and exhaust pressure versus crank angle, for Case 2.

Table 5 – Wall temperature for different regions, for Case 2.

	Temperature
Combustion dome	473 K
Piston	473 K
Cylinder wall	423 K
Intake port wall	311 K
Exhaust port wall	769 K

Table 6 – Initial conditions for different regions of the domain, for Case 2.

Region	Cylinder	Intake	Exhaust
Pressure	0.887 bar	0.684 bar	0.887 bar
Temperature	769 K	311 K	769 K
TKE	3.5 m^2/s^2	3.5 m^2/s^2	3.5 m^2/s^2
Dissipation	300 m^2/s^3	300 m^2/s^3	300 m^2/s^3

4. RESULTS

The results for in cylinder pressure, compared with experimental results, are presented in the following section. It is also presented the CFD results for in cylinder temperature, heat release rate and mass burned fraction compared with values calculated based on in cylinder pressure.

4.1. 2100 RPM, 20% throttle (MAP 0.718 bar), 30° VVT

The results for simulation of engine CFD 3D model running 2100 rpm, 20% throttle (manifold air pressure, MAP, 0.718 bar), 30° VVT are presented in Figure 5. This results are compared to experimental ones obtained at the same conditions that the model boundary conditions are obtained, which is the one the model is running.

In cylinder pressure is presented in Figure 5 (a), in which it can be seen that numerical and experimental results are correlated, once the average difference between CFD and experiment is 0.07 bar where the minimum pressure is 4.7 bar. The average difference is 0.5% for the same interval. Although the in cylinder pressure numerical results is correlated to measured values, the same does not happen to in cylinder temperature, which is presented in Figure 5 (b). From 30 CAD before TDC (330 CAD) until 20 CAD after TDC (380 CAD), the difference between CFD and experimental based temperature is 20%-25% different. Afterwards this difference remains smaller than 5%. It is important to highlight the fact that in cylinder experimental temperature is not a measured value, instead of it is calculated using a 1D model, so the difference between both results can be explained by the difference between both calculation methodologies.

Figure 5 (c) and (d) show the comparison between CFD results and experimental based results for heat release rate and mass burned fraction, both of them presenting considerable difference between numeric and experimental based results. Once again those values are not measured ones but calculated ones based on in cylinder pressure, which is a measured value, still the difference between both results is an indicative that something is not going well on CFD engine model.

Although numeric in cylinder pressure is correlated with measured in cylinder pressure, the other results are not well correlated. The CFD engine model should be slightly modified in order to reduce the differences between those results, although the error might be in the calculation of the experimental temperature. The in cylinder pressure is correlated, what means the numerical model is almost correlated for this case.

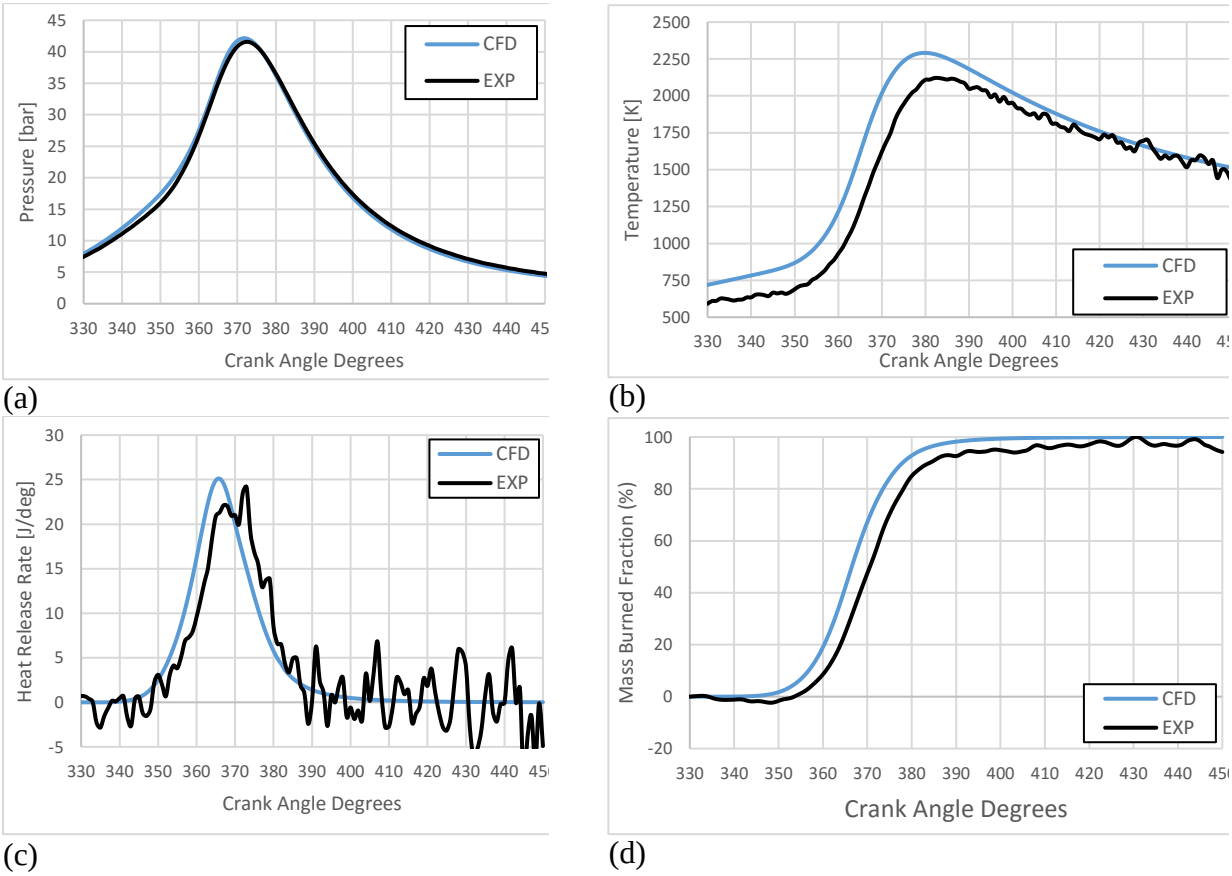

Figure 5 – Engine CFD 3D model results compared with experimental ones for 2100 rpm, 20% throttle (MAP 0.718 bar), 30° VVT. (a) In cylinder pressure CFD and experimental (measured), (b) In cylinder temperature CFD and experimental (calculated), (c) Heat release rate CFD and experimental (calculated), (d) Mass burned fraction CFD and experimental (calculated).

4.2. 2100 RPM , 20% throttle(MAP 0.736 bar), 60° VVT

The results for simulation of engine CFD 3D model running 2100 rpm, 20% throttle (manifold air pressure, MAP, 0.718 bar), 60° VVT are presented in Figure 5. This results are compared to experimental ones obtained at the same conditions that the model boundary conditions are obtained, which is the one the model is running.

In cylinder pressure is presented in Figure 6 (a), in which numerical and experimental results are correlated, the same way it happens for VVT 30°, once the average difference is 0.09 bar in a region where the minimum pressure is 4.5 bar. The average difference between CFD and measured values is 1.1% for the same interval. For this case, good agreement can be observed in Figure 6 (b) for in cylinder temperature between CFD and experimental based values, once the results are well suited except the interval between 10 CAD and 40 CAD after TDC (370 and 400 CAD). For this case, it can be considered that this difference remains in the methodologies of calculation for both models.

Figure 6 (c) and (d) show the comparison between numerical and experimental based results for heat release rate and mass burned fraction, and both charts present good agreement between CFD and experimental based calculation, similarly to temperature. These results indicate the model is well correlated for the case of 2100 rpm, 20% throttle, VVT 60°, once all of the results presented are well fitted.

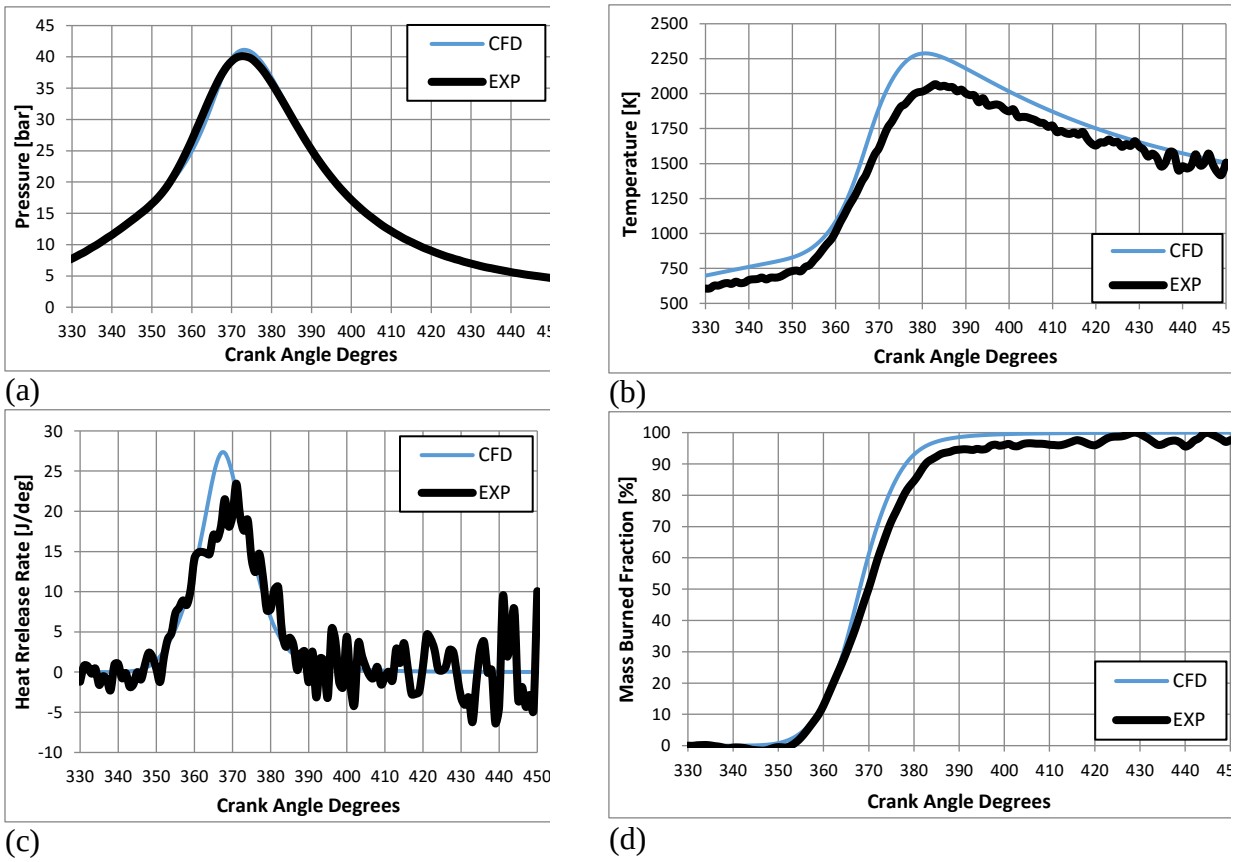

Figure 6 - Engine CFD 3D model results compared with experimental ones for 2100 rpm, 20% throttle (MAP 0.736 bar), 60° VVT. (a) In cylinder pressure CFD and experimental (measured), (b) In cylinder temperature CFD and experimental (calculated), (c) Heat release rate CFD and experimental (calculated), (d) Mass burned fraction CFD and experimental (calculated).

5. CONCLUSIONS

This paper presents the comparison between CFD 3D using ECFM-3Z combustion model and experimental results for two different VVT positions. Results for in cylinder pressure, in cylinder temperature, heat release rate and mass burned fraction are compared in both cases, and both in cylinder pressure comparison show a good correlation between numerical and experimental results, although the other parameters do not correlate well.

Among experimental results evaluated, only in cylinder pressure is a measured value, being the other calculated based on pressure measurement using a thermodynamic model. Once both experimental and numerical results have similar pressure results, it is expected that other results also correlate well.

Among other possibilities, wall temperature values could be evaluated in order to determine its influence in cylinder temperature results, for adjusting temperature and heat release rate and this way, going further this comparison between numerical and experimental results until validation is reached.

6. REFERENCES

Alkidas, A.C., “Combustion advancements in gasoline engines”, Energy Conversion and Management 48(11), 2751-2761, 2007.

Bernard, G., Lebas, R. and Demoulin, F., “A 0D phenomenological model using detailed tabulated chemistry methods to predict diesel combustion heat release and pollutant emissions”, SAE Technical Paper 2011-01-0847, doi: 10.4271/2011-01-0847.

Celik, I.B., Ghia, U., Roache, P.J., Freitas, C.J., Coleman, H.W., and Raad, P.E., “Procedure for estimation and reporting of uncertainty due to discretization in CFD applications”, ASME Journal of Fluids Engineering, Editorial, Vol. 130, No. 7, July 2008, pp. 078001-1 – 078001-4, 4 pages, 2008.

Colin, O., Benkenida, A. and Angelberger, C., “3D Modeling of mixing, ignition and combustion phenomena in highly stratified gasoline engines”, Oil & Gas Science and Technology – Rev. IFP, 58(1), 47-62, 2003.

Colin, O. and Benkenida, A., "The 3-Zones extended coherent flame model (ECFM-3Z) for computing premixed/diffusion combustion", Oil & Gas Science and Technology – Rev. IFP, 59(6), 593-609, 2004.

CD-ADAPCO, "STAR CD Version 4.20: Methodology of Internal Combustion Engine Applications", CD-ADAPCO, 2013.

Drake, M.C. and Haworth, D.C., "Advanced gasoline engine development using optical diagnostics and numerical modelling", Proceedings of the Combustion Institute 31, 99-124, 2007.

Fonseca, L.G. "Caracterização do escoamento de ar em um motor de combustão interna utilizando mecânica dos fluidos computacional", UFMG University, Ms.C. Thesis, Belo Horizonte, 2014.

Ge, H-W., Shi, Y., Reitz, R.D., Wickman, D.D. and Willems, W., "Optimization of a HSDI diesel engine for passenger cars using a multi-objective generic algorithm and multi-dimensional modelling", SAE International Journal of Engines 2, 691-713, 2009, doi: 10.4271/2009-01-0715.

Millo, F., Luisi, S., Borean, F. and Stroppiana, A., "Numerical and experimental investigation on combustion characteristics of a spark ignition engine with an early intake valve closing load control", Fuel 121, 298 – 310, 2014, doi: 10.1016/j.fuel.2013.12. 047.

Pariotis, E.G., Kosmadakis, G.M. and Rakoupoulos, C.D., "Comparative analysis of three simulation models applied on a motored internal combustion engine", Energy conversion and management 60, 45-55, 2012, doi: 10.1016/j.enconman.2011.11. 031.

Poinsot, T. and Veynante, D., "Theoretical and numerical combustion", R.T. Edwards Inc., Philadelphia, 2001.

7. RESPONSIBILITY NOTICE

The following text, properly adapted to the number of authors, must be included in the last section of the paper: The authors are the only responsible for the printed material included in this paper.